



Biogenic Synthesis of Silver Nanoparticles using *Chromolaena odorata* Leaf Extract and its Antioxidant, Antimicrobial, and Anticancer Activities

M. Swarnalatha^{1*}, R. Ragunathan², Jesteena Johney² and R. Vishnupriya²

¹Department of Zoology, Emerald Heights College for Women, Ooty, TN, India

²Department of Biotechnology, Centre for Bioscience and Nanoscience Research, Eachanari, Coimbatore, TN, India

Received: 31.08.2024 Accepted: 22.09.2024 Published: 30.12.2024

*swarnalathaslv@gmail.com



ABSTRACT

An attempt was made in this work to biosynthesize silver nanoparticles (AgNPs) from aqueous leaf extract of *Chromolaena odorata*. Qualitative analysis of phytochemicals revealed the presence of alkaloids, terpenoids, proteins, sterols, quinones, flavonoids, tannins, saponins, and phenolics in the aqueous extract of *C. odorata* leaves. The separation of constituents in the aqueous extract was done using Thin-layer Chromatography. Total flavonoid content, phenolic content, and total antioxidant activity were investigated and were estimated to be 26.43 µg/ml, 63.74 mg/g GAE, and 41.45 µg/ml respectively. The characterization of the synthesized *C. odorata* extract-mediated AgNPs was done by UV-Vis absorption spectroscopy, Fourier Transform Infra-Red Spectroscopy, and Field Emission Scanning Electron Microscopy. The result of antibacterial activity by the Agar well diffusion method showed that all the test isolates were susceptible to the synthesized AgNPs. The MTT assay results demonstrated that the synthesized AgNPs had an antiproliferative impact on the MCF 7 cell line, with IC₅₀ values of 96.34 µg/ml. As confirmed by acridine orange-ethidium bromide staining, AgNPs induced apoptosis in cancer cells. These findings suggest that *C. odorata*-synthesized AgNPs induce apoptosis and inhibit cell growth and proliferation.

Keywords: *Chromolaena odorata*; Silver nanoparticles; Phytochemical analysis; Antioxidant activity; Anticancer activity.

1. INTRODUCTION

Silver nanoparticle synthesis has attracted a lot of attention due to its unique characteristics and emerging uses, especially in the biomedical field. There are physical, chemical, and biological techniques for the synthesis of AgNPs. The biological synthesis method uses plant extracts to synthesize nanoparticles, which is widely used because it is eco-friendly and inexpensive. In this process, the silver ions derived from a precursor such as silver nitrate are reduced to nanoparticles by phytochemicals extracted from plants. This method not only permits the synthesis of nanoparticles quickly but also does not involve any toxic chemicals. Hence, this method is more sustainable and efficient for the synthesis of silver nanoparticles with antimicrobial and catalytic properties.

Chromolaena odorata popularly referred to as Siam weed or fire weed is a perennial herb from the Asteraceae family native to America but also prevalent in tropical and sub-tropical regions of the world. This plant is known for its invasive features and rich phytochemical profile such as flavonoids, phenols, alkaloids, terpenoids, saponins, proteins, and sterols. These phytochemicals are effective in enhancing the plant's medicinal properties

and have been known to cure infections, inflammation, and wounds. The biogenic synthesis of silver nanoparticles using *Chromolaena odorata* utilizes these phytochemicals to enable the conversion of silver ions (Ag⁺) into elemental silver (Ag₀) to form efficient and non-toxic nanoparticles.

Another major benefit of the silver nanoparticles synthesized from *Chromolaena odorata* is its antioxidant properties. Oxidative stress is caused by an imbalance between free radicals and antioxidants in the body, associated with severe disease conditions such as cancer, cardiovascular diseases, and neurodegenerative disorders (Halliwell *et al.* 2015). Silver nanoparticles possess antimicrobial properties; they are useful in medical applications since they can eradicate nearly all types of pathogens such as bacteria, fungi, and viruses. The AgNPs synthesized from *Chromolaena odorata* are highly effective against microbes mainly because of the increased surface area of the NPs and micro-size, thus enhancing their interaction with microbes. The action mechanism incorporates the liberation of silver ions that alter microbial cell membranes, and affect the organism's cellular respiration and DNA synthesis (Rai *et al.* 2009). It has recently been reported that silver nanoparticles possess anticancer

effects. Initial studies suggest that AgNPs have cytotoxic activity against several tumor cell lines, suppress tumor growth, and can also increase the anticancer potency of conventional chemotherapy drugs (Khan *et al.* 2022). The nature of their anticancer properties is thought to be due to the ability of AgNPs to induce Reactive oxygen species (ROS) formation, which results in oxidative stress and ultimate death in cancer cells. The use of silver nanoparticles in wound care has gained attraction due to their antimicrobial and healing-promoting properties. The synthesized AgNPs from *Chromolaena odorata* have exhibited Cell proliferation, improved collagen synthesis, and anti-inflammatory activity for accelerated wound healing. These nanoparticles act as a shield against microbial invasion while at the same time promoting the healing of tissues that have been injured.

Recently, research has focused on creating nanomaterials through nanotechnology methods that align with the principles of green chemistry, aiming to reduce or eliminate the use of harmful chemicals. This has led to a widespread global interest in environment-friendly green nanotechnology-based approaches for producing nanoparticles (Thakkar *et al.* 2010). To demonstrate this alternative approach, the current study aims to synthesize silver nanoparticles with *Chromolaena odorata* leaf extract and evaluate their antioxidant, antimicrobial, anticancer, and wound healing efficiency.

2. MATERIALS AND METHODOLOGY

The primary material was the plant named *Chromolaena odorata* which was collected from Eachanari, Coimbatore, Tamilnadu. Analytical reagent-grade chemicals were used in this study: Silver nitrate (AgNO_3) (Nice chemicals, Cochin), distilled water, and Muller Hinton Agar (Himedia, Mumbai, India). Essential apparatus includes a mortar and pestle for grinding plant material, beakers or flasks for mixing, and a magnetic stirrer to ensure homogenization of the extract with silver nitrate. The characterization studies of the synthesized silver nanoparticle were carried out by several tools, including a UV-Vis spectrophotometer (Labtronics single beam visible UV spectrophotometer-LT 291), FTIR (Shimadzu FTIR Spectrophotometer), and FESEM (ZEISS). The wound healing cell culture plates (typically 6-well or 12-well) were utilized to grow a monolayer of a suitable cell line, CO_2 incubator for incubating the plates, and Phase contrast or fluorescent microscopes were used to capture images of the cells at different periods. Cell culture plates (96 well plates), MCF 7 Cell line, MTT solution, DMSO, and ELISA reader (Robonik-Readwell Touch Elisa Plate Analyser) were used for quantifying the cell viability.

2.1 Extraction and Phytochemical Screening

The *Chromolaena odorata* were gathered from Eachanari, Coimbatore, Tamilnadu. The leaves were dried in a shaded area before the experiment. 1g of the dried leaves was ground using a mortar and pestle and was transferred to two different conical flasks containing 30 ml of distilled water and 30 ml of ethanol. Then, the aqueous solution was heated for 30 minutes at 40 °C while being stirred. The mixture was then allowed to cool to room temperature to be filtered using Whatman No. 1 filtration. Qualitative phytochemical screening was carried out to determine the presence of alkaloids, terpenoids, proteins, sterols, quinones, flavonoids, tannins, saponins, and phenolics (Rajesh *et al.* 2020).

2.2. Antioxidant Activity of the Extract

2.2.1 Total Antioxidant Activity

The total antioxidant activity of the samples was evaluated using the Phospho-molybdenum method (El-Jemli *et al.* 2016). 0.5 ml of the sample aliquot was mixed with 0.5 ml of total antioxidant reaction mixture (0.6 M sulphuric acid, 28 mM sodium phosphate, and 4 mM ammonium molybdate). After being covered, the test tubes were incubated in a water bath for 90 minutes at 50 °C. The absorbance of the mixture was measured at 695 nm after the samples were cooled. The total antioxidant content ($\mu\text{g}/\text{AAEq}$) was calculated using ascorbic acid as the standard.

2.2.2. Total Flavonoid Content

The total flavonoid content was measured spectrophotometrically using the aluminum chloride test (Nguyen *et al.* 2020). 1 ml of the extract was mixed with 0.1 ml of 10% aluminum chloride solution and 0.1 ml of sodium potassium tartrate, followed by 2.8 ml of distilled water. After adding the reagents, the tubes were incubated at room temperature for 30 minutes before being measured at 415 nm using a spectrophotometer (Labtronics LT-291 Spectrophotometer). The blank was kept without the sample, and standard quercetin was used to quantify the mg/g flavonoid concentration.

2.2.3. Total Phenolic Content

Total phenol content was determined by the Folin Ciocalteu reagent assay method. The 1 ml of the extract was mixed with 0.2 ml of 10% Folin Ciocalteu Reagent (FCR) and 1 ml of the 20% Na_2CO_3 solution; the mixture was kept in the water bath at 45 °C for 45 minutes. After incubation, the absorbance value was determined at 765 nm using a UV spectrophotometer. Gallic acid was used to determine the mg/g of the total phenol content (Jaya *et al.* 2019).

2.3 Thin-Layer Chromatographic Analysis of the Plant Extract

Thin-layer Chromatography was an essential method to separate the phytochemical constituents present in the extract (Pitakpawasutthi *et al.* 2016). In this method, a small amount of plant extract was applied to a pre-coated silica gel TLC plate which was developed using a solvent system consisting of Toluene: Ethyl Acetate: Methanol: Ethanol: Acetic acid: Distilled water at a ratio of 3:3:2:1:1:1. The plate was then exposed to iodine chamber for the visualization of the separated compound.

2.4 Biogenic Synthesis of Silver Nanoparticles

1 mM of AgNO₃ was synthesized by suspending 0.01698 g of AgNO₃ in 100 ml of distilled water. Then the silver nanoparticles were synthesized by combining 10 ml of aqueous plant extract and 10 ml of 1 mM AgNO₃ solution. The mixture was then kept in a dark room for 48 hours (Küp *et al.* 2020). After incubation, a color change was observed from light yellow to yellowish-brown color which indicates the formation of *C. odorata* AgNPs which was confirmed by further characterization procedures.

2.5 Characterization of the Silver Nanoparticles

The UV-Vis spectrophotometer measures the maximum absorbance spectra for the nanoparticles which quantifies the size and yield of the synthesized AgNPs. The synthesized AgNPs were evaluated at 300-700 nm wavelength range (Bishoyi *et al.* 2024). The biomolecules in the leaves of *C. odorata* act as reducing agents for silver ions and stabilizers for AgNPs which were analyzed by Fourier Transform Infrared (FTIR) spectrophotometer using KBr powder method in the range of 500–4000 cm⁻¹. Field Emission Scanning Electron Microscopy (FESEM) is a valuable technique employed to visualize the microstructure of materials. In this study, the dried AgNPs were subjected to FESEM analysis to capture the clear surface of AgNPs at magnifications of 50,000 X and 120,000 X (Hasyim *et al.* 2023).

2.6 Antibacterial Activity of the Synthesized Silver Nanoparticles

The antibacterial activity of the synthesized nanoparticles was tested against pathogenic bacteria such as *Escherichia coli*, *Staphylococcus aureus*, *Klebsiella pneumoniae*, and *Pseudomonas aeruginosa*. Mueller Hinton agar media (Himedia, Mumbai) was employed for the antibacterial study (Jaya *et al.* 2019). 39 g of media was dissolved in 1000 ml of distilled water and sterilized at 121 °C at 15 lbs. After pouring and solidification of the media, 70 µl of bacteria were swabbed on the surface of the agar surface with a sterile cotton swab and wells

were lawn with a cork borer. 20 µl of silver nanoparticle, extract, and silver nitrate solutions were added to the respective wells. Azithromycin (15 mcg) was used as the standard antibiotic disc (Himedia, Mumbai). After sample addition, the plates were then incubated at 37 °C for 24 hours. Following the incubation period, the presence of antibacterial activity in the sample was verified by observing the zone of inhibition, measured in mm.

2.7 Cell Cytotoxicity by MTT Assay

The cytotoxicity was assessed by the MTT assay method (Linima *et al.* 2023). MCF-7 Cell Line in DMEM media was allowed to grow in a CO₂ incubator at 5% CO₂, 80% humidity, and 37 °C for 48 hours. After incubation, viable cells were confirmed using an inverted microscope (Unicon). The synthesized AgNPs were taken at different concentrations (12.5, 25, 50, 100, and 200 µg) together with 100 µl of the Cell Line. A control (just Cell Line) was also added and incubated in the CO₂ incubator for 24 hours. The cells were washed with trypsin and DMSO after incubation. A volume of 20 µl of MTT dye was then added, and the optical density (OD) was measured after 24 hours using an ELISA reader (Robonik-Readwell Touch Elisa Plate Analyser) at a wavelength of 570 nm. The value obtained was calculated as a percentage of viable cells compared to negative control. The cell morphology was observed under a phase contrast inverted microscope and the images were captured.

2.8 Apoptosis Induction by Acridine Orange–Ethidium Bromide Staining

Human breast cancer cell line MCF-7 was purchased from NCCS, Pune, India. Approximately a density of 2 x 10⁵ cells/2 ml was seeded in six well plates and treated with the desired concentration of the synthesized silver nanoparticle from *C. odorata*. Then it was incubated at 37 °C for 24 hours in the presence of 5% humidified CO₂. The cells that were attached to the surface were rinsed with 200 µl of PBS followed by trypsinization. Then it was subjected to the staining with acridine orange (AC) (100 µg/mL) and ethidium bromide (Et-Br) (100 µg/ml). 50 µl of the stained cells were immediately examined under a compound microscope with suitable filter settings for fluorescence, with an excitation wavelength of 488 nm, and an emission wavelength of 525 nm for AC, and an excitation wavelength of 560 nm, and an emission wavelength of 645 nm for Et-Br.

3. RESULTS AND DISCUSSIONS

3.1 Phytochemical Analysis

A phytochemical test was carried out for both aqueous and ethanolic plant extracts of *C. odorata*. Both

ethanolic and aqueous extracts tested positive for alkaloids, phenols, tannins, steroids, terpenoids, and flavonoids. Saponins and quinines were only found in the aqueous extract. Phenolics, alkaloids, terpenoids, and cardiac glycosides found in the extracts have been documented to have medicinal properties and health-promoting effects (Liu *et al.* 2004). The qualitative analysis of phytochemicals revealed that *C. odorata* leaf extract has the potential to be a reducing agent due to the presence of secondary metabolites (Table 1).

3.1. Phytochemical Analysis

A phytochemical test was carried out for both aqueous and ethanolic plant extracts of *C. odorata*. Both ethanolic and aqueous extracts tested positive for alkaloids, phenols, tannins, steroids, terpenoids, and flavonoids. Saponins and quinines were only found in the aqueous extract. Phenolics, alkaloids, terpenoids, and cardiac glycosides found in the extracts have been documented to have medicinal properties and health-promoting effects (Liu *et al.* 2004). The qualitative analysis of phytochemicals revealed that *C. odorata* leaf extract has the potential to be a reducing agent due to the presence of secondary metabolites (Table 1).

Table 1. Qualitative Phytochemical Screening for Aqueous and Ethanolic leaf extracts of *Chromolaena odorata*

Phytochemicals	Aqueous Extract	Ethanolic Extract
Alkaloids	+	+
Terpenoids	+	+
Phenols	+	+
Sugar	-	-
Saponins	+	-
Flavonoids	+	+
Quinines	+	-
Proteins	+	-
Steroids	+	+

3.2 Antioxidant Studies of the Extract

Evaluations of antioxidant activities of *C. odorata* plant extracts often include the determination of Total phenolic content (TPC), Total flavonoid content (TFC), and Total antioxidant activity (TAA). These parameters are important in determining the ability of the plant to neutralize free radicals and prevent the oxidative stress, associated with chronic diseases. The antioxidant potential of the plant extract revealed that *C. odorata* plant extracts contained a large amount of antioxidant content. The total antioxidant content in aqueous extract was estimated to be 49.45 $\mu\text{g/ml}$ while the ethanolic extract contains 61.45 $\mu\text{g/ml}$ antioxidant content. Plant polyphenols have been shown in several studies to have potential antioxidant properties, which are particularly effective in preventing diseases linked to oxidative stress

(Nguyen *et al.* 2020). The total phenolic content for aqueous and ethanol was 49.85 and 63.74 GAE/mg respectively. Flavonoid contents for aqueous and ethanol were estimated to be 40.23 and 26.43 $\mu\text{g/ml}$, respectively. The ethanolic extracts from *C. odorata* leaves were higher than those of the aqueous extract. The determination of the total phenolic content, total flavonoid content, and total antioxidant activity suggest that *Chromolaena odorata* has a high potential as an antioxidant agent from natural sources. Fig. 1 shows the antioxidant activities of the plant extracts.

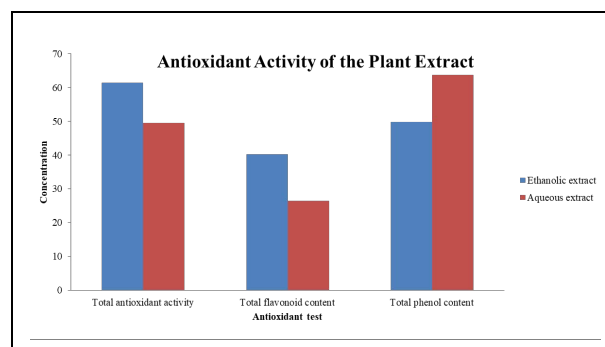


Fig. 1: Antioxidant activity of *C. odorata* leaves

3.3 Thin Layer Chromatography of the Extracts

TLC profiles can reveal whether phytochemicals are present in the samples. After adding six absolute solvents as mobile phase both the aqueous and ethanolic extracts showed a total of two spots, respectively. The obtained R_f values ranged from 0.61 to 0.93. The aqueous extracts yielded the highest R_f value. Various solvent systems produced distinct phytochemicals based on the determined R_f values. This is because various solvent polarities could isolate different groups of compounds (Cowan *et al.* 1999). In this study, the aqueous extract produced R_f values of 0.62 and 0.93 while the ethanolic extract produced R_f values of 0.6 and 0.90 which were thought to contain the secondary flavonoid content. According to earlier research conducted by (Oh *et al.* 2010), the range of R_f values for flavonoids in *C. odorata* extracts is 0.5 to 0.9.

3.4 Silver Nanoparticle Synthesis from *C. odorata*

The first indication of the presence of AgNPs was a color shift with time. As soon as plant extract was added to the AgNO_3 solution, the mixture turned brown (Fig. 2). Bioreduction of silver ions in the plant extract was confirmed by the colloidal solution's color change. The dark brown color of the colloidal solution was due to the Surface plasmon resonance (SPR), which is the collective oscillation of AgNPs' free electrons. The synthesized AgNPs' color shift from pale yellow to dark brown was in line with the findings of other published reports (Javed *et al.* 2016).

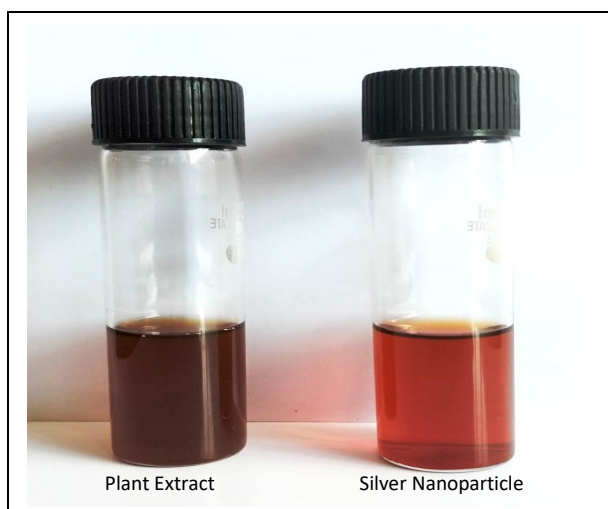


Fig. 2: Visual observation of the formation of *C. odorata* Silver NPs

3.5. Characterization Studies of the Nanoparticles

The UV absorption spectrum of the AgNPs that were synthesized using *C. odorata* leaf extract is displayed in Fig. 3a. A narrow line at a shorter wavelength denotes a smaller particle size, while a broad peak at a higher wavelength indicates a bigger particle size (Hasyim *et al.* 2023). A band of absorption between 300 and 700 nm was measured. The synthetic AgNPs' maximum absorption for the *C. odorata* aqueous leaf extract was 450 nm. It was found that the absorption spectra, which were also gradually increasing, were influenced by the longer incubation period. The measurement findings showed a maximum absorbance of around 450 nm with a single narrow SPR peak, confirming the presence of spherical and monodisperse AgNPs. An SPR peak between 400 and 500 nm shows the existence of silver nanoparticles (Sherin *et al.* 2020). The SPR peak value or wavelength indicates the approximate size. Characterization with a UV-Vis spectrophotometer revealed a constant absorbance as a function of time and no peak shift, indicating the high production and stability of AgNPs. The flavonoids and phenolic phytochemicals in the plant extract may be the primary reducing and capping agents for AgNPs formation. Several investigations indicated that flavonoid is the primary molecule responsible for reducing and capping AgNPs (Alomar *et al.* 2020). Fig. 3 b displays the Fourier Transform Infrared (FTIR) spectra of bio-reduced silver nanoparticles, obtained between 500 and 4000 cm^{-1} . This analytical approach effectively identified the various functional groups in the silver nanoparticles synthesized from leaf extracts.

The FTIR spectrum of the silver nitrate (AgNO_3) precursor showed discrete peaks at 1635.64 cm^{-1} and a broad peak at 3348.42 cm^{-1} . According to Nandiyanto *et al.* (2019), these peaks correspond to the

carbonyl stretch of amides, the triple-linked carbon, and the stretching vibration of the O-H functional group. Fig. 3 c displays the FESEM picture of *C. odorata*-AgNPs. The theoretical estimate of particle size is based on the assumption that particles are spherical (Siddiqi *et al.* 2018). In this investigation, the observed shapes range from spherical to triangular to decahedral.

Numerous parameters influence the structure of synthesized nanoparticles, including extract concentration, contact time, pH, and silver salt concentration. The FESEM image showed an excellent separation between the AgNPs, which could be attributed to the capping effect of the *C. odorata* extract. This explains the narrow SPR band shape, which is a feature of well-dispersed AgNPs. The particle sizes ranged from 2 to 29 nm, with an average of 28.36 nm.

3.6 Evaluation of Antibacterial Activity

The antibacterial activity of AgNPs was investigated against *Escherichia coli*, *Staphylococcus aureus*, *Klebsiella pneumoniae*, and *Pseudomonas aeruginosa*. The study's positive controls were Azithromycin whereas the negative controls were DMSO. Fig. 4 depicts the diameter of the AgNP inhibition zone; the results show antibacterial action against the tested organism. Furthermore, *P. aeruginosa* bacteria were more sensitive to synthesized AgNPs than the other tested bacteria, which could be attributed to differences in bacterial cell wall structure. The antibacterial action caused by a simultaneous process like penetration of AgNPs in the cell wall of bacteria leads to cellular content leakage (Rajesh *et al.* 2020) and silver ion release.

3.7 Cytotoxicity Effect of AgNP Against MCF-7 Cell Line

The MTT test was used to assess the cytotoxicity of synthesized AgNPs in MCF-7 cells at various concentrations (12.5, 25, 50, 100, and 200 $\mu\text{g/mL}$). The synthesized AgNPs had a dose-dependent influence on cell viability, with values of 49.21% at the greatest concentration (200 $\mu\text{g/mL}$) and 96.48% at the lowest concentration (12.5 $\mu\text{g/mL}$) (Fig. 5). The IC50 value for synthesized AgNPs was estimated to be 96.34%. Moreover, inverted microscopy was used to analyze the morphology of MCF-7 cells treated with synthesized AgNPs for 24 hours. The control cells had a normal morphology; they adhered to the surface and grew by roughly 100%. In the MCF-7 cells treated with synthesized AgNPs, cell death was visible.

The loss of cell adhesion, smaller and denser cells, and decreased cell size were further indications of cell shrinkage. *C. odorata* contains a high concentration of flavonoid glycosides, which may play a role in the reduction process of synthesized AgNPs, contributing to

their cytotoxic effect, flavonoid glycosides have the potential to promote cell death by activating the autophagy pathway, generating ROS, and causing apoptosis. Apoptosis is a prominent cause of cell death

when exposed to AgNPs synthesized from a plant extract (Farah *et al.* 2016). Khan *et al.* (2022) suggest that additional characteristics may contribute to NP-induced cell death.

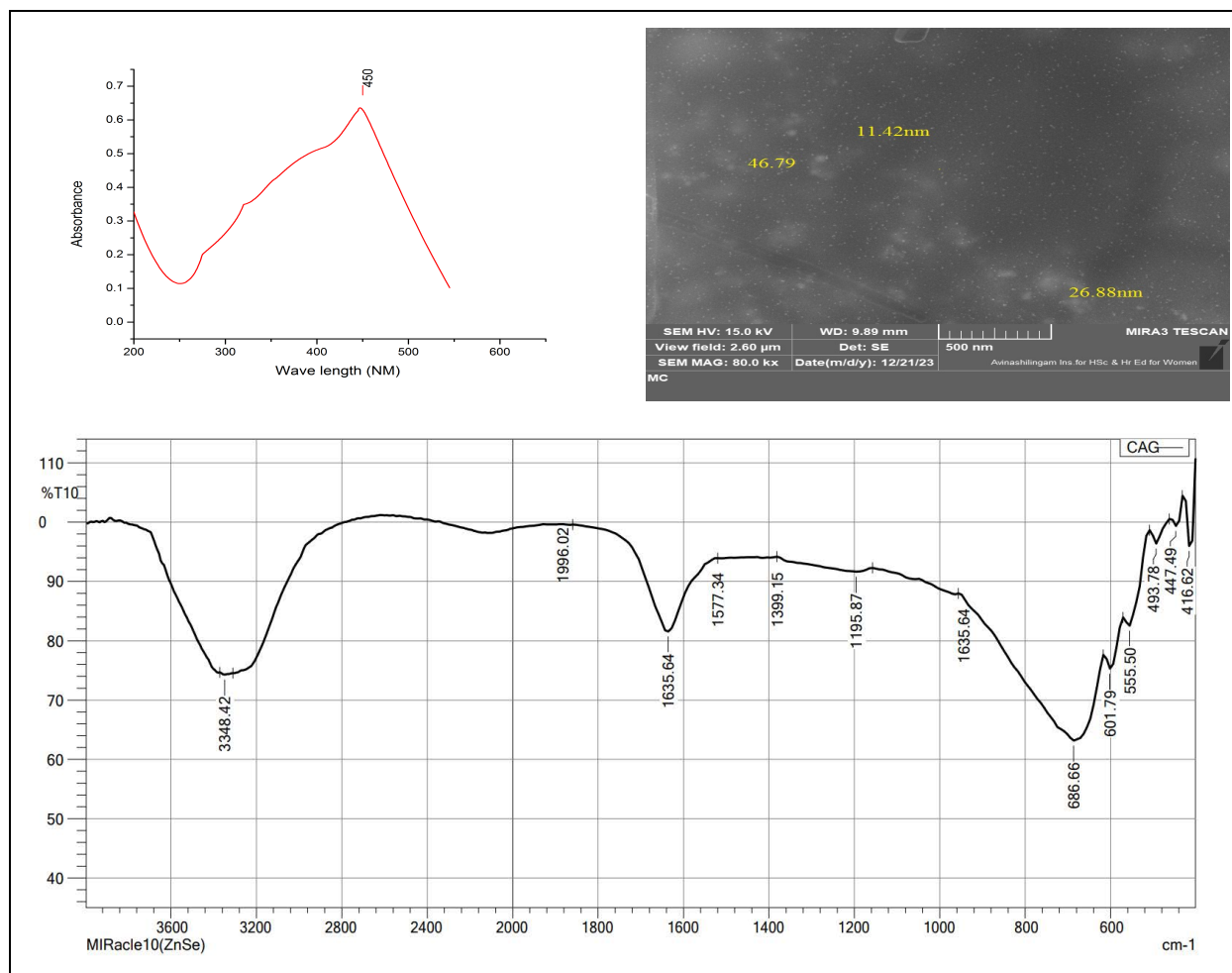


Fig. 3: Characterization of Silver NPs using *C. odorata* leaf extracts: (a) UV Absorption spectrum of AgNPs, (b) SEM Microscopic view of AgNPs, and (c) FTIR spectrum of AgNPs

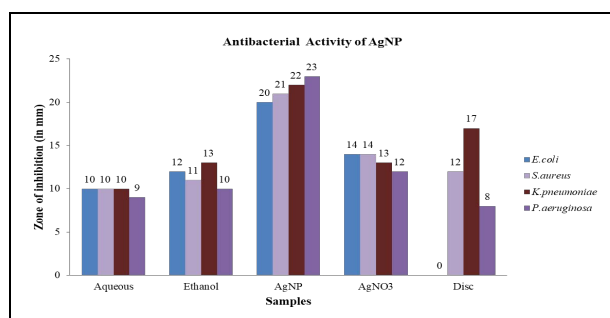


Fig. 4: The Zone of Inhibition (mm) of aqueous, ethanol and AgNPs of *C. odorata*

3.8 Apoptosis Study for Synthesized AgNP

To determine if the increase in cell death was caused by apoptosis, MCF-7 cells were exposed to *C.*

odorata-synthesized AgNPs for 24 hours and stained with acridine orange and ethidium bromide. Untreated MCF-7 cells had approximately 92.2% viability. AO stain (green fluorescence) was evenly distributed in these cells, with normal nuclear morphology without red fluorescence (Fig. 6a).

All treated samples showed a significant drop in viable cell percentage. In contrast, all treatments resulted in a large increase in apoptotic cells, as indicated by the number of red-colored cells. According to (Li *et al.* 2018), cells treated with AgNPs may cause altered autophagy, which leads to the build-up of damage to organelles like mitochondria and can cause oxidative stress, inflammation, and DNA damage. The study's findings were determined to be in line with earlier reports by (Farah *et al.* 2016; Buttacavoli *et al.* 2018).

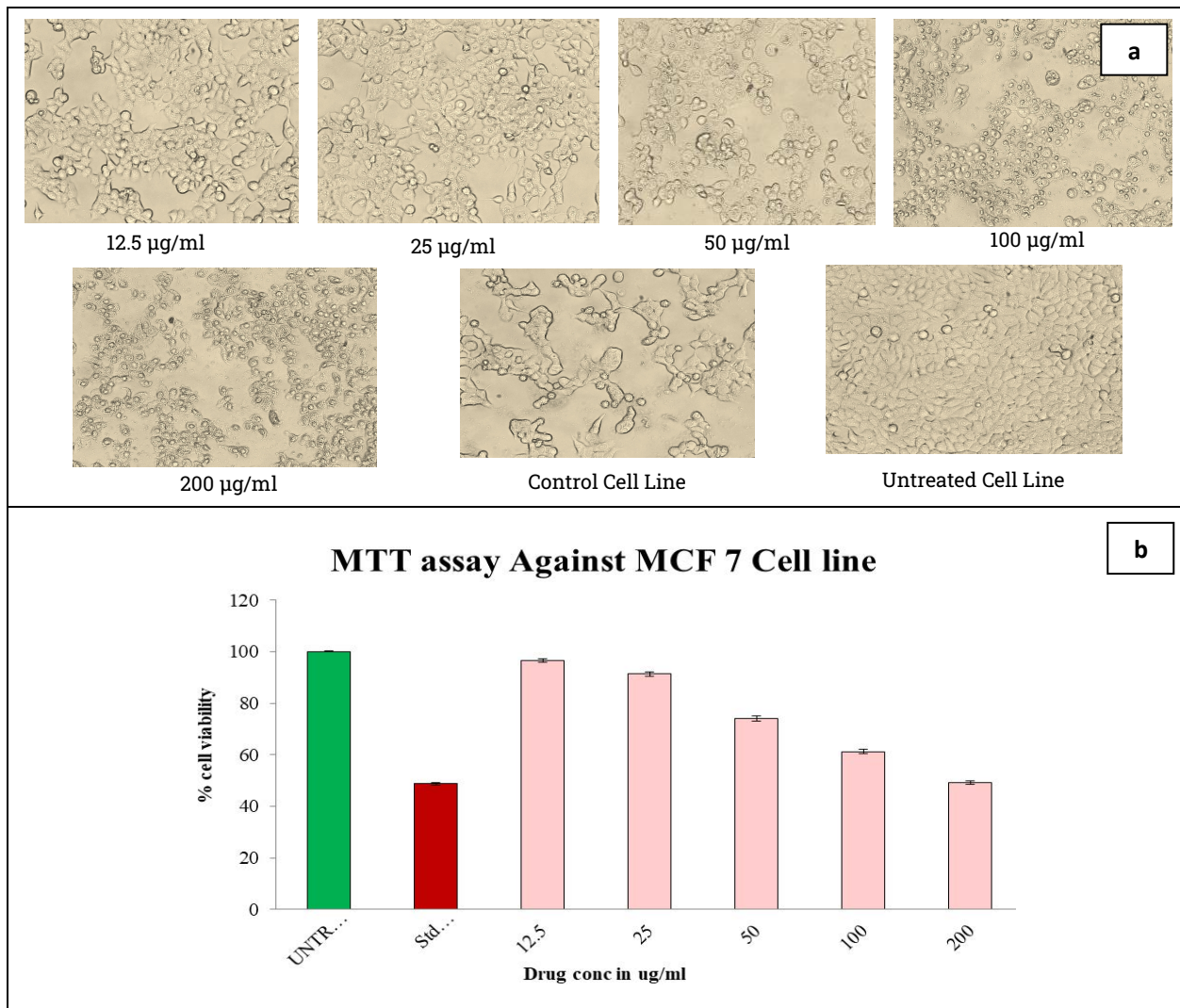


Fig. 5: Cytotoxicity assay by MTT method: (a) Morphological changes on MCF-7 cells at different concentrations of AgNP, and (b) Percentage of cell viability of MCF-7

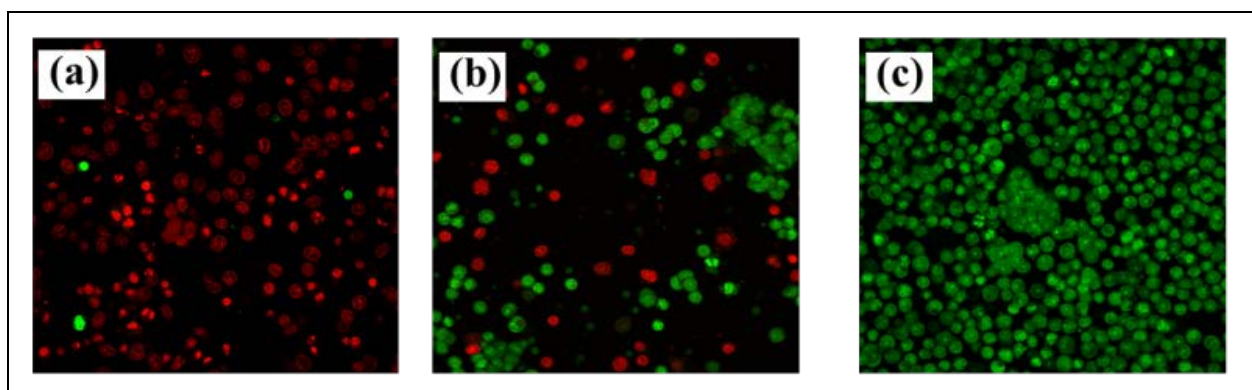


Fig. 6: The Impact of nanosilver treatments on apoptosis and necrosis in MCF-7 cells: (a) Treated sample, (b) Standard sample, and (c) Untreated sample

4. CONCLUSION

This study successfully synthesized an aqueous extract of *C. odorata*-mediated silver nanoparticles. The extract's phytochemicals were screened, and flavonoids, alkaloids, saponins, proteins, and phenols were discovered in the *C. odorata* leaf extract. The total phenolic content of *C. odorata* was measured to be 63.74 and 49.85 µgGAE/mg, while the flavonoid content was found to be 40.23 and 26.43 µgQE/mg. An additionally, the antioxidant activity of the plant was determined to be 61.45 and 49.45 µg/ml Ascorbic acid. These results indicate that *C. odorata* exhibits high antioxidant activity and contains various phenolic compounds that could be utilized to treat diseases caused by free radicals. AgNPs have been reported to have a surface plasmon resonance (SPR) band at 450 nm. Aside from that, the formation of *C. odorata*-AgNPs was examined using FESEM. FESEM micrographs revealed that *C. odorata* -AgNPs had a variety of shapes, including spherical, triangular, and decahedral, with minimal agglomerations. This study shows that *C. odorata* leaf extracts might successfully heal wounds by inhibiting the in vitro growth of *P. aeruginosa*. When appropriately used, *C. odorata* leaf extracts could be a source of active antimicrobial compounds for the development of medicines against *P. aeruginosa* infections. MCF-7 cell viability was reduced in a dose-dependent manner when exposed to *C. odorata*-synthesized AgNPs. *C. odorata*-derived AgNPs also increased intracellular ROS levels and accelerated autophagy and apoptosis. When crude plant extract is utilized as a reducing agent for AgNP production, the phytochemicals from *C. odorata* boost its anticancer properties. Because of their increased bio-availability and compatibility, biosynthesized AgNPs have a significant potential for usage in therapeutic applications for chronic disorders, including cancer.

ACKNOWLEDGEMENT

The authors would like to thank the Management of Centre for Bioscience and Nanoscience Research, Eachanari, Coimbatore, Tamilnadu, India (Affiliated to Bharathiar University and recognized by DSIR-SIRO) for providing the laboratory and infrastructural facilities and support; in addition, the authors convey special thanks to Dr. R. Raguathan, Director of CBNR for his constant support and for providing us the opportunity to publish the research work in the scientific community.

FUNDING

This research received no specific grant from any funding agency in the public, commercial, or not-for-profit sectors.

CONFLICTS OF INTEREST

The authors declare that there is no conflict of interest.

COPYRIGHT

This article is an open-access article distributed under the terms and conditions of the Creative Commons Attribution (CC BY) license (<http://creativecommons.org/licenses/by/4.0/>).



REFERENCES

- Alomar, T. S., AlMasoud, N., Awad, M. A., El-Tohamy, M. F. and Soliman, D. A., An eco-friendly plant-mediated synthesis of silver nanoparticles: Characterization, pharmaceutical and biomedical applications, *Mater. Chem. Phys.*, 249, 123007 (2020).
<https://doi.org/10.1016/j.matchemphys.2020.123007>
- Bishoyi, A. K., Sahoo, C. R., Samal, P., Mishra, N. P., Jali, B. R., Khan, M. S. and Padhy, R. N., Unveiling the antibacterial and antifungal potential of biosynthesized silver nanoparticles from *Chromolaena odorata* leaves, *Sci. Rep.*, 14(1), 7513 (2024).
<https://doi.org/10.1038/s41598-024-57972-5>
- Buttacavoli, M., Albanese, N. N., Di Cara, G., Alduina, R., Faleri, C., Gallo, M., Pizzolanti, G., Gallo, G., Feo, S., Baldi, F. and Cancemi, P., Anticancer activity of biogenerated silver nanoparticles: an integrated proteomic investigation, *Oncotarget*, 9(11), 9685–9705 (2018).
<https://doi.org/10.18632/oncotarget.23859>
- Cowan, M. M., Plant Products as Antimicrobial Agents, *Clin. Microbiol. Rev.*, 12(4), 564–582 (1999).
<https://doi.org/10.1128/CMR.12.4.564>
- El-Jemli, M., Kamal, R., Marmouzi, I., Zerrouki, A., Cherrah, Y. and Alaoui, K., Radical-Scavenging Activity and Ferric Reducing Ability of *Juniperus thurifera* (L.), *J. oxycedrus* (L.), *J. phoenicea* (L.) and *Tetraclinis articulata* (L.), *Adv. Pharmacol. Sci.*, 2016, 1–6 (2016).
<https://doi.org/10.1155/2016/6392656>
- Farah, M. A., Ali, M. A., Chen, S. M., Li, Y., Al-Hemaid, F. M., Abou-Tarboush, F. M., Al-Anazi, K. M. and Lee, J., Silver nanoparticles synthesized from *Adenium obesum* leaf extract induced DNA damage, apoptosis and autophagy via generation of reactive oxygen species, *Colloids Surf., B*, 141, 158–169 (2016).
<https://doi.org/10.1016/j.colsurfb.2016.01.027>

- Halliwell, B. and Gutteridge, J. M. C., *Free Radicals in Biology and Medicine*, Oxford University Press, (2015).
<https://doi.org/10.1093/acprof:oso/9780198717478.01.0001>
- Hasyim, S. and John, A., Green Synthesis of Silver Nanoparticles Using Leaves of *Chromolaena odorata* and its Antioxidant Activity, *J. Trop. Life Sci.*, 13(2), 305–310 (2023).
<https://doi.org/10.11594/jtls.13.02.08>
- Javed, I., Hussain, S. Z., Shahzad, A., Khan, J. M., Ur-Rehman, H., Rehman, M., Usman, F., Razi, M. T., Shah, M. R. and Hussain, I., Lecithin-gold hybrid nanocarriers as efficient and pH selective vehicles for oral delivery of diacerein—In-vitro and in-vivo study, *Colloids Surfaces B Biointerfaces*, 141, 1–9 (2016).
<https://doi.org/10.1016/j.colsurfb.2016.01.022>
- Jaya, P. M., Ragunathan, R. and Josteena, J., Evaluation of bioactive compounds from Jasminum polyanthum and its medicinal properties, *J. Drug Deliv. Ther.*, 9(2), 303–310 (2019).
<https://doi.org/10.22270/jddt.v9i2.2413>
- Khan, Y., Sadia, H., Ali Shah, S. Z., Khan, M. N., Shah, A. A., Ullah, N., Ullah, M. F., Bibi, H., Bafakeeh, O. T., Khedher, N. Ben, Eldin, S. M., Fadhl, B. M. and Khan, M. I., Classification, Synthetic, and Characterization Approaches to Nanoparticles, and Their Applications in Various Fields of Nanotechnology: A Review, *Catalysts*, 12(11), 1386 (2022).
<https://doi.org/10.3390/catal12111386>
- Küp, F. Ö., Çoşkunçay, S. and Duman, F., Biosynthesis of silver nanoparticles using leaf extract of *Aesculus hippocastanum* (horse chestnut): Evaluation of their antibacterial, antioxidant and drug release system activities, *Mater. Sci. Eng. C*, 107, 110207 (2020).
<https://doi.org/10.1016/j.msec.2019.110207>
- Li, W., Ma, G., Wu, Q., Liu, Y., Liu, X. and Wang, J., Withdrawn: Effects of clinicopathological factors on prognosis of young patients with breast cancer, *Oncotarget, Medicine (Baltimore)*, 100(5), 1-8 (2021).
<https://doi.org/10.18632/oncotarget.24062>
- Linima, V. K., Ragunathan, R. and Johny, J., Biogenic synthesis of RICINUS COMMUNIS mediated iron and silver nanoparticles and its antibacterial and antifungal activity, *Heliyon*, 9(5), e15743 (2023).
<https://doi.org/10.1016/j.heliyon.2023.e15743>
- Liu, R. H., Potential Synergy of Phytochemicals in Cancer Prevention: Mechanism of Action, *J. Nutr.*, 134(12), 3479S-3485S (2004).
<https://doi.org/10.1093/jn/134.12.3479S>
- Rajesh, M. K., Muralikrishna, K. S., Nair, S. S., Krishna, K. B., Subramaniya, T. M., Sonu, K. P., Subaharan, K., Sweta, H., Keshava, P. T. S., Neeli, C., Karunasagar, I., Hebber, K. B. and Karun, A., Facile coconut inflorescence sap mediated synthesis of silver nanoparticles and its diverse antimicrobial and cytotoxic properties, *Mater. Sci. Eng. C*, 111, 110834 (2020).
<https://doi.org/10.1016/j.msec.2020.110834>
- Nandiyanto, A.B.D., Oktiani, R. and Ragadhita, R., How to Read and interpret FTIR Spectroscopy of Organic Nano-material, *Indones. J. Sci. Technol.*, 4(1): 97–118 (2019).
<https://doi.org/10.17509/ijost.v4i1.15796>
- Nguyen, V. T., Nguyen, M. T., Nguyen, N. Q. and Truc, T. T., Phytochemical Screening, Antioxidant Activities, Total Phenolics and Flavonoids content of Leaves from *Persicaria odorata* Polygonaceae, *IOP Conf. Ser. Mater. Sci. Eng.*, 991(1), 012029 (2020).
<https://doi.org/10.1088/1757-899X/991/1/012029>
- Oh, D. Y., Talukdar, S., Bae, E. J., Imamura, T., Morinaga, H., Fan, W., Li, P., Lu, W. J., Watkins, S. M. and Olefsky, J. M., GPR120 Is an Omega-3 Fatty Acid Receptor Mediating Potent Anti-inflammatory and Insulin-Sensitizing Effects, *Cell*, 142(5), 687–698 (2010).
<https://doi.org/10.1016/j.cell.2010.07.041>
- Pitakpawasutthi, Y., Thitikornpong, W., Palanuvej, C. and Ruangrunsi, N., Chlorogenic acid content, essential oil compositions, and in vitro antioxidant activities of *Chromolaena odorata* leaves, *J. Adv. Pharm. Technol. Res.*, 7(2), 37 (2016).
<https://doi.org/10.4103/2231-4040.177200>
- Rai, M., Yadav, A. and Gade, A., Silver nanoparticles as a new generation of antimicrobials, *Biotechnol. Adv.*, 27(1), 76–83 (2009).
<https://doi.org/10.1016/j.biotechadv.2008.09.002>
- Sherin, L., Sohail, A., Amjad, U.-S., Mustafa, M., Jabeen, R. and Ul-Hamid, A., Facile green synthesis of silver nanoparticles using Terminalia bellerica kernel extract for catalytic reduction of anthropogenic water pollutants, *Colloid Interface Sci. Commun.*, 37, 100276 (2020).
<https://doi.org/10.1016/j.colcom.2020.100276>
- Siddiqi, K. S., Husen, A. and Rao, R. A. K., A review on biosynthesis of silver nanoparticles and their biocidal properties, *J. Nanobiotechnol.*, 16(1), 14 (2018).
<https://doi.org/10.1186/s12951-018-0334-5>
- Thakkar, K. N., Mhatre, S. S. and Parikh, R. Y., Biological synthesis of metallic nanoparticles, *Nanomedicine Nanotechnol., Biol. Med.*, 6(2), 257–262 (2010).
<https://doi.org/10.1016/j.nano.2009.07.002>